

A brief study of instabilities in the context of space magnetohydrodynamic simulations

Um breve estudo de instabilidades no contexto de simulações de magneto-hidrodinâmica espacial

Edgard de F.D. Evangelista*, Margarete O. Domingues, Odim Mendes, Oswaldo D. Miranda

Instituto Nacional de Pesquisas Espaciais, São José dos Campos, SP, Brasil.

Recebido em 17 de agosto de 2015. Aceito em 8 de setembro de 2015

The study of the hydrodynamic instabilities in the context of the magnetohydrodynamics (MHD) is very important in many branches of physics. Particularly, we can mention geophysical and astrophysics, where we have several processes involving hydrodynamic effects, such as shock waves, plasma flows and the propagation of waves. In these scenarios it is frequent the onset of instabilities. For example, let a system be formed by two phases with different densities and relative velocities. Besides, consider these phases are in contact with each other by means of a tangential surface, that is, an interface where there is no transference of matter and where there are only relative tangential velocities. In this case, under certain circumstances, we will have a particular type of phenomenon, the so-called Kelvin-Helmholtz (KH) instability. In this paper we will address to the basic theory of such instabilities, explaining how they arise from the hydrodynamic equations and showing the numerical simulation of a particular case. Besides, we show examples of other MHD instabilities which are usually found in astrophysical processes.

Keywords: magnetohydrodynamics, instabilities, FLASH Code.

O estudo das instabilidades hidrodinâmicas no contexto da magneto-hidrodinâmica (MHD) é muito importante para várias áreas da física. Particularmente, podemos mencionar a geofísica e a astrofísica, em que temos diversos processos envolvendo efeitos hidrodinâmicos, tais como ondas de choque, fluxos de plasma a propagação de ondas. Nestes cenários é frequente o surgimento de instabilidades. Por exemplo, seja um sistema formado por duas fases com diferentes densidades e velocidades relativas. Além disso, considere que estas fases estão em contato entre si por meio de uma superfície tangencial, isto é, uma interface onde não há transferência de matéria e onde há somente velocidades relativas tangenciais. Nesse caso, sob certas circunstâncias, teremos um tipo particular de fenômeno, conhecido como instabilidade de Kelvin-Helmholtz (KH). Nesse artigo abordaremos a teoria básica de tais instabilidades, explicando como elas surgem das equações hidrodinâmicas e mostrando a simulação numérica de um caso particular. Além disso, são mostrados exemplos de outras instabilidades em MHD, as quais são geralmente encontradas em processos astrofísicos.

Palavras-chave: magnetohidrodinâmica, instabilidades, código FLASH.

1. Introduction

Magnetohydrodynamics consists in the study of the fluids which are compressible and conductor of electricity under the influence of magnetic fields. Roughly speaking, the equations governing the behavior of these fluids under such conditions are obtained through the combination of the Euler equa-

tions of the fluid mechanics with the Maxwell equations of the electromagnetism.

The formalism of the MHD is of great interest for several branches of physics, such as space geophysics, astrophysics and engineering. For example, the MHD is applicable in many scenarios in astrophysics and cosmology, once most of the baryonic matter in the universe is formed by plasma, including stars and interplanetary, interstellar and inter-

*Endereço de correspondência: edgard.evangelista@inpe.br.

galactic media. Besides, many astrophysical systems are not in local thermodynamic equilibrium, which requires an extra kinematic treatment for the complete description of the phenomena. Particularly, solar winds and blasts are understood under the framework of the MHD.

Concerning the instabilities, let a system be initially at a stationary state, that is, the variables which define its configuration do not depend on time. If that system undergo small perturbations, which are gradually smoothed such that there are not appreciable deviation from the stationary state, we can say such a system is stable [1]. On the other hand, if we imagine the system undergo small deviation in a given region of its domain, in such a manner the acting forces tend to increase more and more the deformations, we have an unstable configuration. Such an unstable behavior can occur in several forms, that is, there are many types of instabilities, having particular characteristics.

According to [2], there is a diversity of dynamic instabilities which are characteristic of fluids. For example, a static fluid in a gravitational field can undergo convective inversions when its inferior portion is heated or its superior portion is cooled. Generally speaking, a vertical stratification in the density profile can be caused by a temperature gradient, yielding the so-called Rayleigh-Taylor (RT) instabilities [3]. Further, the presence of a radiation field with spatially variable opacity can induce unstable temperature and density distributions.

Of particular interest is the case where the fluid has two adjacent phases with different densities and which have a tangential movement relative to each other. In this case, at the interface between the phases, under certain circumstances, we can have the KH instabilities. Such instabilities came from the combined effect of the pressure, the gravity and the Reynolds strain.

In this paper we address to the MHD and to its instabilities, particularly the KH type. The basic formalism of the MHD is treated in Section 2; in Section 3 we discuss some examples in the context of space physics where the phenomena related to the MHD play important roles; in Section 4 we focus on the KH instabilities and we show the simulation of a particular case using FLASH Code; next, we present our conclusions. Besides, in Annex A there is a brief discussion on FLASH Code.

2. Basic formalism of the MHD

The ideal MHD describes the interplay between a magnetic field and a compressible fluid, with no viscosity and which is a perfect conductor of electricity (hence the term “ideal”) [4]. Besides, we consider the fluid has a non-relativistic behavior, that is, at any point of the domain and at any instant, the velocities are small when compared to the speed of light in vacuum.

In general, the model which describes the phenomena related to that interaction is built through the combination of the equations governing the fluid dynamics and the Maxwell equations of the electromagnetism. It is worth bearing in mind the Maxwell equations yields an extra expression for the time evolution of the magnetic field, besides imposing a constraint to the model. Such a constraint is given by Gauss’s Law for magnetism and it is stated as: the divergence of the magnetic field is zero at all points of the domain.

Following the scheme shown in [5], the system of equations which form the ideal MHD model in three dimensions contains:

- conservation of mass (1 equation);
- conservation of momentum (3 equations);
- Faraday’s Law (3 equations);
- conservation of energy (1 equation).

These eight equations are expressed in terms of eight dependent variables:

- mass density (ρ);
- components x , y and z of the momentum density (ρu_x , ρu_y , ρu_z), where u_x , u_y , u_z are the components of the velocity;
- components x , y and z of the magnetic field (B_x , B_y , B_z);
- plasma total energy (E),

where

$$E = \rho e + \rho \frac{\mathbf{u} \cdot \mathbf{u}}{2} + \frac{\mathbf{B} \cdot \mathbf{B}}{2\mu_0}. \quad (1)$$

In Eq. (1) the energy density e is given by the equation of state of an ideal gas:

$$e = \frac{p}{(\gamma - 1)\rho}, \quad (2)$$

where p is the pressure. In the subsequent sections we will briefly describe the above-mentioned equations.

2.1. Conservation of mass

This equation will have the usual form used in the fluid mechanics, namely:

$$\frac{\partial \rho}{\partial t} + \nabla \cdot (\rho \mathbf{u}) = 0. \tag{3}$$

2.2. Conservation of momentum

Written in differential form, the conservation of momentum has the form Ref. [5]

$$\frac{\partial \rho \mathbf{u}}{\partial t} + \nabla \cdot (\rho \mathbf{u} \mathbf{u} + p \mathbf{I}) = \mathbf{j} \times \mathbf{B}, \tag{4}$$

where \mathbf{I} the 3×3 unit matrix. In our case, Ampère-Maxwell law is written as $\nabla \times \mathbf{B} = \mu_0 \mathbf{j}$, such that Eq. (4) assumes the form

$$\frac{\partial \rho \mathbf{u}}{\partial t} + \nabla \cdot (\rho \mathbf{u} \mathbf{u} + p \mathbf{I}) = \frac{1}{\mu_0} (\nabla \times \mathbf{B}) \times \mathbf{B}; \tag{5}$$

now, using the vectorial identity $(\nabla \times \mathbf{B}) \times \mathbf{B} = (\mathbf{A} \cdot \nabla) \mathbf{B} - (\nabla \mathbf{B}) \cdot \mathbf{A}$, Eq. (5) is written as

$$\begin{aligned} \frac{\partial \rho \mathbf{u}}{\partial t} + \nabla \cdot \left[\rho \mathbf{u} \mathbf{u} + \left(p + \frac{B^2}{2\mu_0} \right) \mathbf{I} - \frac{\mathbf{B} \mathbf{B}}{\mu_0} \right] \\ = -\frac{1}{\mu_0} \mathbf{B} \nabla \cdot \mathbf{B}. \end{aligned} \tag{6}$$

2.3. Faraday's law

In integral form, Faraday's law is written as

$$-\frac{d}{dt} \iint_S \mathbf{B} \cdot d\mathbf{S} = \oint_{\partial S} \mathbf{E} \cdot d\mathbf{l}, \tag{7}$$

where the surface S is bounded by the closed curve ∂S , \mathbf{E} is the electric field and $d\mathbf{l}$ is the line element.

However, we are considering the fluid moves relative to some inertial frame, in such a way we have to consider a form of Eq. (7) which is consistent with such a scenario. First, following Ref. [6], the total rate of change of the magnetic flux through S is given by

$$\begin{aligned} \frac{d}{dt} \iint_S \mathbf{B} \cdot d\mathbf{S} &= \iint_S \frac{\partial \mathbf{B}}{\partial t} \cdot d\mathbf{S} + \oint_{\partial S} \mathbf{B} \times \mathbf{u} \cdot d\mathbf{l} \\ &+ \iint_S (\nabla \cdot \mathbf{B} \mathbf{u}) \cdot d\mathbf{S}, \end{aligned} \tag{8}$$

where the third term in the right side is due to the movement of S through the inhomogeneous vector

field in which the magnetic field-lines are generated. Substituting Eq. (8) in Eq. (7), using Stokes' theorem, considering that \mathbf{E} is zero in the comoving frame (once in that frame the total variation of \mathbf{B} is zero) and doing the necessary algebra, we have

$$\frac{\partial \mathbf{B}}{\partial t} + \nabla \cdot (\mathbf{u} \mathbf{B} - \mathbf{B} \mathbf{u}) = -\mathbf{u} \nabla \cdot \mathbf{B}. \tag{9}$$

2.4. Conservation of energy

Conservation of the hydrodynamic energy

$$E = \rho \frac{p}{(\gamma - 1)\rho} + \rho \frac{\mathbf{u} \cdot \mathbf{u}}{2}, \tag{10}$$

considering a fixed volume of fluid, is given by

$$\frac{\partial E}{\partial t} + \nabla \cdot [\mathbf{u}(E + p)] = \mathbf{j} \cdot \mathbf{E}. \tag{11}$$

where \mathbf{j} is the current density. On the other hand, we can write the term $\mathbf{j} \cdot \mathbf{E}$ in the form

$$\begin{aligned} \mathbf{j} \cdot \mathbf{E} &= \frac{1}{\mu_0} \left\{ \mathbf{B} \cdot \frac{\partial \mathbf{B}}{\partial t} - (\mathbf{u} \cdot \mathbf{B}) \nabla \cdot \mathbf{B} \right. \\ &\left. - \nabla \cdot [(\mathbf{B} \cdot \mathbf{B}) \mathbf{u} - (\mathbf{u} \cdot \mathbf{B}) \mathbf{B}] \right\}, \end{aligned} \tag{12}$$

which was deduced from Ampère's law, combined with the vector identities

$$\nabla \cdot (\mathbf{X} \times \mathbf{Y}) = \mathbf{Y} \cdot (\nabla \times \mathbf{X}) - \mathbf{X} \cdot (\nabla \times \mathbf{Y}) \tag{13}$$

$$\mathbf{E} \times \mathbf{B} = (\mathbf{B} \cdot \mathbf{B}) \mathbf{u} - (\mathbf{u} \cdot \mathbf{B}) \mathbf{B}, \tag{14}$$

valid for arbitrary vectors \mathbf{X} , \mathbf{Y} and where \mathbf{E} , \mathbf{B} are the magnetic and electric fields, respectively.

Finally, using Eq. (1) the equation of the energy E becomes

$$\begin{aligned} \frac{\partial E}{\partial t} + \nabla \cdot \left[\left(E + p + \frac{\mathbf{B} \mathbf{B}}{2\mu_0} \right) \mathbf{u} - \frac{1}{\mu_0} (\mathbf{u} \cdot \mathbf{B}) \mathbf{B} \right] \\ = -\frac{1}{\mu_0} (\mathbf{u} \cdot \mathbf{B}) \nabla \cdot \mathbf{B}. \end{aligned} \tag{15}$$

The reader should note that, so far, we addressed to the ideal MHD. However, strictly speaking, the ideal version of the formalism is only applicable when the plasma is strongly collisional, such that the energy distributions of the particles can be considered Maxwellian and the resistivity due to such collisions is negligible. In other words, the ideal MHD is basically a set of conservation laws.

On the other hand, the non-ideal forms of the MHD are those which include dissipative and entropy terms, where there is the onset of effects such as resistivity, viscosity, radiation transport and thermal conduction.

Among those non-ideal models, it is worth emphasizing the resistive MHD, once it is a useful formalism in the study of some fundamental questions concerning the phenomena observed on Earth's magnetosphere [7]. Besides, the finite resistivity is omnipresent in real systems, in such a way that resistive diffusion cannot be neglected in several cases [8].

Specifically, in the framework of resistive MHD, it is possible to understand the phenomenon known as magnetic reconnection. Following [8], a simple way of picturing such an effect is considering two magnetic field lines being carried with the fluid and obeying to the flux conservation law. When these field lines come close together at some point of the fluid, they are cut and undergo reconnection, assuming a different shape, where such an effect of "cut-and-reconnect" is due to the finite resistivity. During the process, the magnetic energy is released in the form of thermal and kinetic energy. It is worth pointing out that almost all nonlinear processes in MHD involve such reconnections.

3. Examples of application of the MHD

3.1. RT instabilities in Crab nebula

Now, it would be interesting to discuss some cases in the context of space physics, where phenomena related to the MHD are important. First, we mention the onset of the RT instabilities in supernovae, more specifically in Crab nebula [9]. Such a nebula, which is the remnant of the supernova explosion recorded by Chinese and Arab astronomers in 1054, is located 2000 parsecs away in the constellation of Taurus.

Today, Crab nebula is still expanding at a rate of nearly 1450 km s^{-1} and it shows a luminosity of $8 \times 10^4 L_{\odot}$ (where $L_{\odot} = 3.8 \times 10^{26} \text{ W}$ is the luminosity of the Sun [10].) A large proportion of the radiation being emitted comes from relativistic electrons spiralling around strong magnetic fields. The continuous source of the electrons and the permanence of the high luminosities remained as a major problem in astrophysics until the discovery of a pulsar at the center of Crab nebula [10].

In fact, the object inside Crab nebula belongs to the class of pulsar wind nebula (PWN), which consists of a nebula powered by the wind of a pulsar. Such a wind is formed by charged particles accelerated at relativistic velocities, where the source of their energy are the strong magnetic fields generated by the spinning pulsar. The high pressures of that hot plasma inflated by the pulsar produces a shock wave into the cooler exterior remnants of the supernova.

The nature of the contact between the pulsar wind and the remnants has a configuration similar to the one where a heavier (denser) fluid is placed above a lighter (less dense) one in a gravitational field. As it was mentioned, such configuration is subject to the onset of the RT instabilities.

Figure 1 shows the phenomenon in the simulation of a supernova. The instabilities are those peculiar structures in the form of "fingers" or "trees", which arise when the shock waves from the heavier layers penetrate the overlying lighter shells. Other figures, related to Crab nebula itself, can be found in [9].

3.2. Magnetorotational (MR) instabilities in accretion disks

The large viscosities observed in accretion disks have for a long time remained a fact difficult to explain. Molecular viscosity alone, as well as convection and tidal mixing, were too weak to explain such

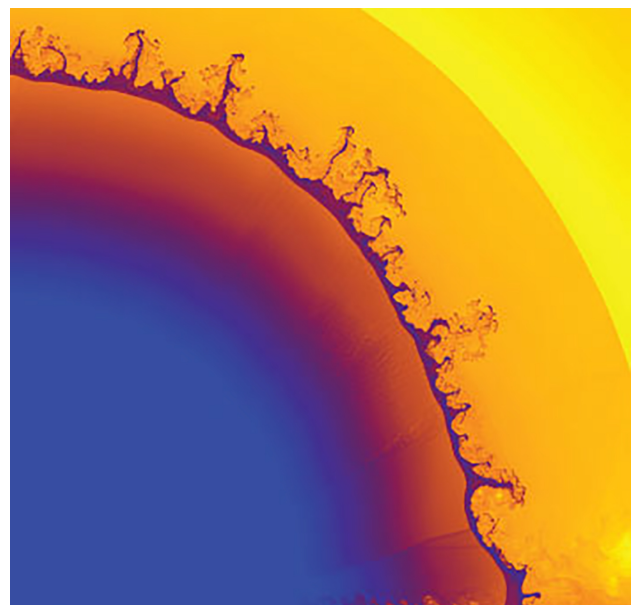


Figure 1: This simulation shows the RT instabilities during a supernova in a red supergiant star.

a behavior. However, in the paper [11], the authors demonstrated that the MR instabilities are present in accretion disks, which could explain the turbulent mixing necessary to the onset of the observed mass accretion rates.

Basically, the developing of the MR instabilities occurs in scenarios where there is a weak magnetic field normal to the plane of the disk and the disk itself is in differential rotation ($d\Omega/dR < 0$.)

In ideal plasma, the magnetic field links contiguous fluid portions that are situated along a same field line. In this case, the magnetic field lines are “frozen” in the fluid portions, that is, the movement of the fluid carries the magnetic field attached to him. So, we can think of the magnetic force acting on the fluid as springs attaching two given fluid elements.

In order to understand the basic mechanism of formation of the MR instabilities, consider a system where we have two masses connected by a spring. Besides, such masses are in differential rotation, where the inner mass has a higher angular velocity than the outer one.

Initially, consider the two bodies are separated by a given distance; then, the differential rotation increases the displacement, and the spring tension causes the inner mass to slow down and the outer one to speed up; consequently, there is transfer of angular momentum from the inner to the outer mass, where the inner migrates inwards and the outer is pushed outwards; the cycle is repeated, but this time starting with a longer displacement.

A particular case is where the magnetic fields are strong. In such a scenario, the cycle described above will not occur. Instead, the tension will cause the oscillation in the displacement between the bodies.

Figures 2 and 3 show the simulation of the MR instability in a disk. In fact, the authors used a square box to represent a small part of the disk. They consider that a given gravitational source is located at a position $x \ll 0$, and the disk is in Keplerian rotation. The colors show the density (which decreases from red to black) and the lines represent the constant magnetic field.

Figure 2 shows the initial configuration ($t = 0$ s), while in Fig. 3 we have the simulation at the instant $t = 5$ s. We can note the growth of the instabilities, where the inner magnetic lines move inwards and the outer ones move outwards. In the reference given in Fig. 2, the reader can find an instructive movie of the simulation.

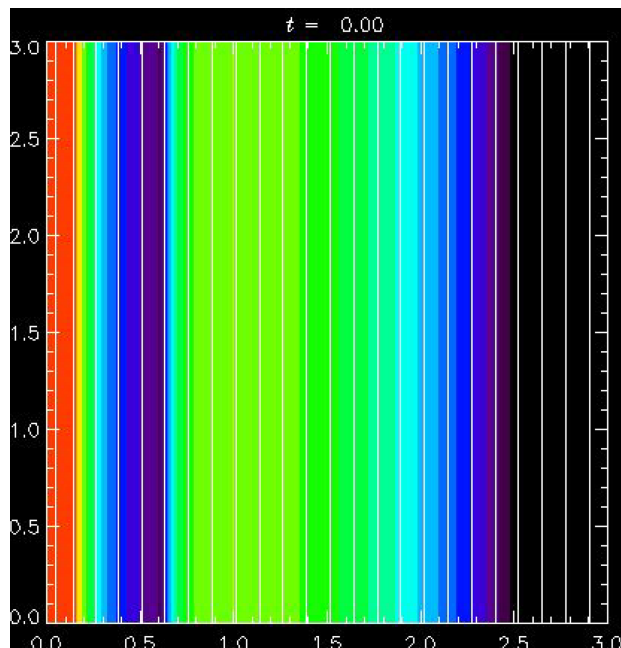


Figure 2: This simulation shows the MR instabilities in an accretion disk. Here we have the initial configuration.

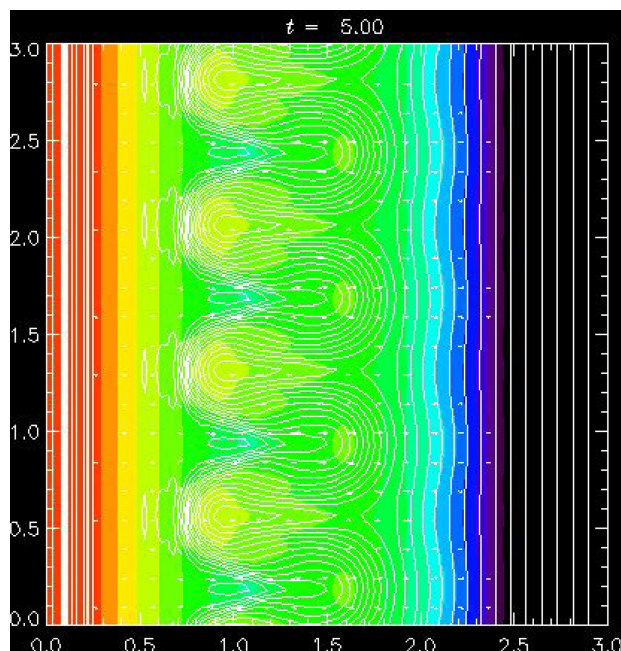


Figure 3: Same as in Fig. 2 for $t = 5$ s.

3.3. Magnetospheric substorms

Earth’s magnetosphere is the region above the ionosphere that is governed by the geomagnetic field and shaped by its interaction with the surrounding interplanetary plasma and field, that is, the solar wind.

Its outer boundary is the magnetopause, a current layer that, to lowest order, separates the geomagnetic field from the solar wind. The shocked solar wind flowing around the magnetosphere outside the magnetopause forms the magnetosheath. By means of the impact of the solar wind, the dayside magnetosphere is compressed, while the nightside is expanded, forming a magnetotail which has several hundreds of Earth's radii. In the magnetotail we have nearly antiparallel magnetic field lines, which encloses a current sheet of hot plasma [7]. Besides, it is worth mentioning the cusps, which are the funnel-shaped regions that contain field lines approaching the vicinity of the magnetopause. Such regions are depicted in Fig. 4.

Earth's magnetosphere has many dynamic features, where one of the most important are the so-called magnetospheric substorms. Although it is not a conclusive fact, one believes that the occurrence of magnetic reconnection in the magnetosphere is related to such substorms.

When the interplanetary magnetic field in the bow-shock region has a southward component (the reader should interpret "southward" as downward in Fig. 4), we have reconnection between the solar wind and the northward directed magnetospheric field, where the arriving particles enter and modify the shape and the composition of the magnetosphere [12].

Once the solar-wind particles gain energy and enter the magnetosphere, they can have two behaviors: in the first, called *directly driven process*, the particles follow immediately to the cusps of the dipole field; in the second mechanism, called *loading-unloading process*, there is a flux of particles

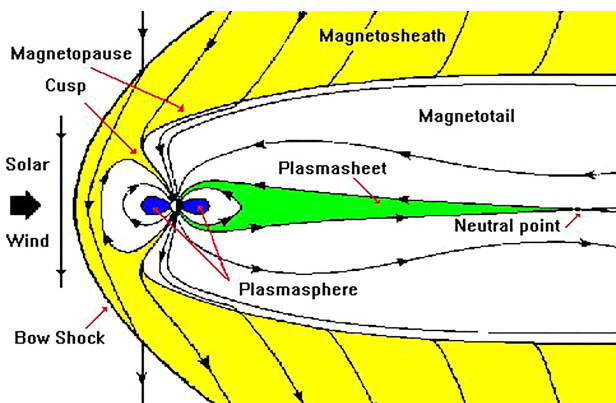


Figure 4: Scheme of Earth's magnetosphere and its main parts.

to the magnetotail, where they are further energized before precipitating into Earth's atmosphere via the so-called substorm current wedge centered near the midnight sector. In both cases, the substorms cause observable effects such as aurora and strong ionospheric currents.

4. Study of the KH instability

According to [13], the KH instabilities arise when one considers the patterns of equilibrium of a stratified heterogeneous fluid whose layers are in relative movement.

First, consider a given incompressible fluid. For the sake of simplicity, let us disregard the viscosity, in such a way Euler's equation for that system takes the form

$$\rho \frac{\partial u_i}{\partial t} + \rho u_i \frac{\partial u_i}{\partial x_j} = -\frac{\partial p}{\partial x_i}, \quad (16)$$

which was written in indicial notation for convenience, where u_i are the components of the velocity at a given point of the fluid, ρ is the density, p is the pressure and x_i ($i=1,2,3$) are the spatial coordinates. Further, consider the flow occurs only in the direction of x and with velocity U , which will be treated as a function of the height z .

Now, consider a given point of the fluid has density, pressure and initial velocity given, respectively, by ρ , p and $\mathbf{v} = (U, 0, 0)$. Suppose that, under the effect of a perturbation, those variables assume the values $\rho + \delta\rho$, $p + \delta p$ e $\mathbf{v}' = (U + u, v, w)$, in such a way Eq. (16) assumes the form

$$(\rho + \delta\rho) \frac{\partial u_i}{\partial t} + (\rho + \delta\rho) \left[(U + u) \frac{\partial u_i}{\partial x} + v \frac{\partial u_i}{\partial y} + w \frac{\partial u_i}{\partial z} \right] = -\frac{\partial}{\partial x_i} (p + \delta p), \quad (17)$$

where we introduced the notation $x_1 = x$, $x_2 = y$ e $x_3 = z$.

If we take $U = U(z)$, $u = u(t,x)$, $u \ll U$, $\delta\rho \ll \rho$ and $\delta p \ll p$, Eq. (17) for $i = 1$ assumes the simplified form:

$$\rho \frac{\partial u}{\partial t} + \rho U \frac{\partial u}{\partial x} + \rho w \frac{\partial U}{\partial z} = -\frac{\partial}{\partial x} \delta p. \quad (18)$$

Similarly, for $i = 2$ and taking $v = v(t,x)$, we have

$$\rho \frac{\partial v}{\partial t} + \rho U \frac{\partial v}{\partial x} = -\frac{\partial}{\partial y} \delta p. \quad (19)$$

At this point it would be straight to deduce the equation for $i = 3$ in the same form we made for ($i = 1$) and $i = 2$. However, we are considering the system is under the effect of the terrestrial gravitational field; besides, we are considering the system is heterogeneous, in the sense that there will be discontinuities along the z direction. Thereby, the corresponding equation for $i = 3$ will take the form [13]

$$\rho \frac{\partial w}{\partial t} + \rho U \frac{\partial w}{\partial x} = -\frac{\partial}{\partial z} \delta p - g \delta \rho + \sum_s T_s \left[\left(\frac{\partial^2}{\partial x^2} + \frac{\partial^2}{\partial y^2} \right) \delta z_s \right] \delta(z - z_s), \quad (20)$$

which is similar to the ones corresponding to ($i = 1$) and ($i = 2$), but with extra terms corresponding to the influence of the gravitational field g and of the surface tensions T_s at the interfaces between the layers. Here, z_s are the z coordinates of the discontinuities.

Besides Eq. (16) and its particular cases described above, we should take into account the continuity equation, written as

$$\frac{\partial \rho}{\partial t} + \frac{\partial}{\partial x_j} (\rho u_j) = 0 \implies \quad (21)$$

$$\frac{\partial \rho}{\partial t} + u_j \frac{\partial \rho}{\partial u_j} = -\rho \frac{\partial u_j}{\partial x_j}.$$

The left side of the second equation is the total derivative of the density, in such a way that if we are considering the case of an incompressible fluid, we have to establish

$$\partial u_j / \partial x_j \equiv \nabla \cdot \mathbf{v} = 0, \quad (22)$$

that is, the velocity field is solenoidal.

Using the same conditions and approximations considered in the previous deductions, Eq. (21) assumes the form

$$\frac{\partial}{\partial t} (\rho + \delta \rho) + (U + u) \frac{\partial}{\partial x} (\rho + \delta \rho) \quad (23)$$

$$+ v \frac{\partial}{\partial y} (\rho + \delta \rho) + w \frac{\partial}{\partial z} (\rho + \delta \rho) = 0. \quad (24)$$

Taking $\rho = \rho(z)$ and $\delta \rho = \delta \rho(t, x)$, we have

$$\frac{\partial}{\partial t} \delta \rho + U \frac{\partial}{\partial x} \delta \rho = -w \frac{\partial \rho}{\partial z} \nabla \cdot \mathbf{v} = 0. \quad (25)$$

So far, we deduced five equations which are necessary for the study of the KH instabilities. However,

as it will be clear subsequently, it is interesting to include an expression which yields the w component of the perturbed velocity at the discontinuities.

Suppose in the perturbed states the interface between two layers becomes slightly deformed, in such a way that the coordinate z_s assume the value

$$z_s + \delta z_s(x, y, t). \quad (26)$$

Defining $w(z_s)$ as the total derivative of Eq. (26), considering z_s constant and following a method similar to the one used in the previous deductions, we have

$$w(z_s) \equiv \frac{D}{Dt} (z_s + \delta z_s) = \frac{\partial}{\partial t} \delta z_s + U \frac{\partial}{\partial x} \delta z_s. \quad (27)$$

4.1. Solution of the equations

Equations (18), (19), (20), (25), (27) and (22) form the system governing the KH instabilities. Following [13], we can initially consider the solutions which depend on x, y and t in the form

$$\exp i(k_x x + k_y y + nt), \quad (28)$$

so that such equations yield

$$i\rho(n + k_x U)u + w\rho \frac{dU}{dz} = -ik_x \delta p; \quad (29)$$

$$i\rho(n + k_x U)v = -ik_y \delta p; \quad (30)$$

$$i\rho(n + k_x U)w = -\frac{d}{dz} \delta p - g \delta \rho - k^2 \sum_s T_s \delta z_s \delta(z - z_s); \quad (31)$$

$$i(n + k_x U) \delta \rho = -w \frac{d\rho}{dz}; \quad (32)$$

$$i(n + k_x U_s) \delta z_s = -w_s; \quad (33)$$

$$i(n + k_y v) = -\frac{dw}{dz}, \quad (34)$$

where $k^2 = k_x^2 + k_y^2$. Multiplying Eqs. (29) and (30) for $-ik_x$ e $-ik_y$ respectively, summing them and considering Eq. (34), we have

$$i\rho(n + k_x U) \frac{dw}{dz} - i\rho k_x w \frac{dU}{dz} = -k^2 \delta p. \quad (35)$$

On the other hand, combining the third, fourth and fifth equations, we have

$$i\rho(n + k_x U)w = -\frac{d}{dz} \delta p - i g \frac{w}{n + k_x U} \frac{d\rho}{dz} + ik^2 \sum_s T_s \left(\frac{w}{n + k_x U} \right) \delta(z - z_s). \quad (36)$$

Eliminating δp between Eqs. (35) and (36), we obtain

$$\frac{d}{dz} \left(\rho(n + k_x U) \frac{dw}{dz} - \rho k_x w \frac{dU}{dz} \right) - k^2 \rho(n + k_x U) w = gk^2 \left\{ \frac{d\rho}{dz} - \frac{k^2}{\rho} \sum_s T_s \delta(z - z_s) \right\} \frac{w}{n + k_x U}. \quad (37)$$

Once the fluid is confined between two surfaces of coordinates $z = 0$ and $z = d$, we must ensure that Eq. (37) satisfies the boundary conditions $w(0) = 0$ and $w(d) = 0$; besides, it is necessary to establish that the factor $w/(n + k_x U)$ is continuous at the interfaces.

Integrating Eq. (37) between $z_s - \varepsilon$ and $z_s + \varepsilon$ and applying the limit $\varepsilon \rightarrow 0$ in the result, we obtain

$$\Delta_s \left\{ \rho(n + k_x U) \frac{dw}{dz} - \rho k_x w \frac{dU}{dz} \right\} = gk^2 \left\{ \Delta_s(\rho) - \frac{k^2}{g} T_s \right\} \left(\frac{w}{n + k_x U} \right)_s, \quad (38)$$

where we defined the notation $\Delta_s(f) = f_{z=z_s^+} - f_{z=z_s^-}$.

We can consider Eq. (38) valid at the interfaces, while in the regions where $z \neq z_s$ we have

$$\frac{d}{dz} \left[\rho(n + k_x U) \frac{dw}{dz} - \rho k_x w \frac{dU}{dz} \right] - k^2 \rho(n + k_x U) w = gk^2 \frac{d\rho}{dz} \frac{w}{n + k_x U}, \quad (39)$$

which follows from Eq. (37).

4.2. Some particular cases

Let us consider initially the case of a system formed by two homogeneous fluids of densities ρ_1 and ρ_2 which have a horizontal relative movement and are separated by the surface $z = 0$. In order to ensure the stability of the system, consider the density ρ_2 of the upper fluid is less than the density ρ_1 of the lower one. Further, the fluids have velocities U_1 and U_2 relative to the laboratory.

In each of the two fluids, the following equation is valid:

$$\left(\frac{d^2}{dz^2} - k^2 \right) w = 0, \quad (40)$$

which was obtained as a particular case of Eq. (39) when one considers ρ and U constant.

Considering the general solution of Eq. (40) is a linear combination of the functions e^{kz} and e^{-kz} ,

bearing in mind the $w(z)$ cannot increase exponentially in both sides of the surface and remembering $w/(n + k_x U)$ must be continuous in such a region, we have the solutions

$$\begin{cases} w_1 = A(n + k_x U_1) e^{kz} & \text{for } z < 0 \\ w_2 = A(n + k_x U_2) e^{-kz} & \text{for } z > 0. \end{cases} \quad (41)$$

Substituting the solutions given by Eqs. (41) in Eq. (38) and considering the value of w at the interface is given by $w_s = A(n + k_x U)$, we have

$$\rho_2(n + k_x U_2)^2 + \rho_1(n + k_x U_1)^2 = gk \left[(\rho_2 - \rho_1) + \frac{k^2 T}{g} \right]. \quad (42)$$

Defining the new variables $\alpha_1 = \rho_1/(\rho_1 + \rho_2)$ and $\alpha_2 = \rho_2/(\rho_1 + \rho_2)$, substituting them in Eq. (42) and expanding the resulting expression, we have

$$n^2 + 2k_x(\alpha_1 U_1 + \alpha_2 U_2)n + k_x^2(\alpha_1 U_1^2 + \alpha_2 U_2^2) - gk \left[(\alpha_1 - \alpha_2) + \frac{k^2 T}{g(\rho_1 + \rho_2)} \right] = 0. \quad (43)$$

Equation (43) is of second order in n , such that its roots are calculated by

$$n = -k_x(\alpha_1 U_1 + \alpha_2 U_2) \pm \left\{ gk \left[(\alpha_1 - \alpha_2) + \frac{k^2 T}{g(\rho_1 + \rho_2)} \right] - k_x^2 \alpha_1 \alpha_2 (U_1 - U_2)^2 \right\}^{1/2} \quad (44)$$

From Eq. (44) we can analyze some particular cases. First, let us investigate the influence of the surface tension T_s on the behavior of the instabilities.

4.3. The surface tension is zero

If we consider $T = 0$ in Eq. (43), we get

$$n = -k_x(\alpha_1 U_1 + \alpha_2 U_2) \pm \left\{ gk(\alpha_1 - \alpha_2) - k_x^2 \alpha_1 \alpha_2 (U_1 - U_2)^2 \right\}^{1/2} \quad (45)$$

For the perturbations which are transverse to the relative movement of the phases, that is, those perturbations where $k_x = 0$, Eq. (45) simplifies to

$$n = \pm \sqrt{gk(\alpha_1 - \alpha_2)}. \tag{46}$$

How in this case n does not depend on U_1 and U_2 , we conclude the instabilities which are transverse to the direction of the flux are not affected by the flux itself.

On the other hand, for an arbitrary direction, there will be stability if the root at the right side of Eq. (44) is real, that is, we will observe instabilities if

$$k_x^2 \alpha_1 \alpha_2 (U_1 - U_2)^2 > gk(\alpha_1 - \alpha_2). \tag{47}$$

Doing $k_x \cong k$ in Eq. (47), we conclude the instabilities will occur for the perturbations which have wave numbers greater than the minimum value given by

$$k_{\min} = \frac{gk(\alpha_1 - \alpha_2)}{\alpha_1 \alpha_2 (U_1 - U_2)^2}. \tag{48}$$

It is worth mentioning that instabilities can arise even when $|U_1 - U_2|$ is small, since the perturbations have wave lengths sufficiently small.

4.4. The effect of the surface tension

We can verify from Eq. (43) that, in the case where $T \neq 0$, there will be instabilities if

$$\alpha_1 \alpha_2 (U_1 - U_2)^2 < g \left\{ \frac{\alpha_1 - \alpha_2}{k} + \frac{kT}{g(\rho_1 + \rho_2)} \right\}. \tag{49}$$

The right side of Eq. (49) will have a minimum when

$$\frac{\alpha_1 - \alpha_2}{k^2} = \frac{T}{g(\rho_1 + \rho_2)}, \tag{50}$$

from which we can calculate k for this particular case, what will be written as k_* . Substituting this value of k in Eq. (50), we have

$$(U_1 - U_2)^2 < \frac{2}{\alpha_1 \alpha_2} \sqrt{\frac{gT(\alpha_1 - \alpha_2)}{\rho_1 + \rho_2}}. \tag{51}$$

The condition given by Eq. (51) establishes that the surface tension will suppress the instabilities if it is true.

4.5. Example

Following [13], consider the air immediately above the sea surface has density $\rho_2 = 1.225 \text{ kg m}^{-3}$. Besides, let us take the values $\rho_1 = 1020 \text{ kg m}^{-3}$ and $T = 7.4 \times 10^{-3} \text{ N m}^{-1}$ for the density and surface tension of the seawater, respectively. Further, the gravitational acceleration at the local has the value $g = 9.81 \text{ m s}^{-2}$, such that Eq. (51) yields

$$|U_1 - U_2| < 6.50 \text{ m s}^{-1}. \tag{52}$$

When $|U_1 - U_2|$ reaches its maximum allowed value, that is, when the system is about to develop instabilities, we will have (using the relation given by Eq. 50)

$$k_* = 36.8 \text{ m}^{-1} \rightarrow \lambda_* = \frac{2\pi}{k_*} = 0.0171 \text{ m}. \tag{53}$$

Now, applying Eq. (49) in Eq. (44) and considering, for the sake of simplicity, $U_1 = 0$, we will have

$$n = \alpha_2 k_* |U_2| = 3.02 \text{ s}^{-1}, \tag{54}$$

once in this case $|U_1 - U_2| = |U_2|$.

Thereby, we conclude that, if the air velocity relative to the sea surface is greater than the value given by Eq. (52), the KH instabilities will manifest themselves in the form of surface waves of length $\lambda_* = 0.0171 \text{ m}$ and velocity given by $n/k_* = 8.2 \times 10^{-3} \text{ m s}^{-1}$.

4.6. A more complex example performed with the FLASH Code

FLASH code (see Annex 1 for details) allows the user to choose the particular values of the parameters concerning each simulation, as well as the forms and values of the physical quantities to be used. Thereby, we defined a model which has the initial configuration such that its time evolution leads to the appearance of KH instabilities.

Following [14], we configured a domain with the dimension $[0, 1] \times [-1, 1] \text{ cm}$ in which the physical quantities are given by Table 1, where ρ is the density, p is the pressure, $\mathbf{v} = (v_x, v_y, v_z)$ is the velocity in each point of the fluid and $\mathbf{B} = (B_x, B_y, B_z)$ is the magnetic field. Besides, these quantities are given in CGS units, once this system is commonly used in the FLASH code.

Roughly speaking, the codes intended to deal with MHD problems use Riemann solvers in order

Table 1: Initial data for the KH instabilities problem [14].

physical quantity	value/form (in CGS units)
ρ	1.0
B_x	1.0
B_y	0.0
B_z	0.0
p	50.0
u_x	$5[\tanh(20y + 10) - \tanh(20y - 10) - 1.0]$
u_y	$0.25 \sin(2\pi x)[e^{-100(y+0.5)^2} - e^{-100(y-0.5)^2}]$
u_z	0.0

to handle the equations. Particularly, FLASH code permits the users to choice some of such methods, namely: the Roe scheme (named after Phil Roe [15]), HLL (Harten-Lax-van Leer [16]), HLLC (Harten-Lax-van Leer-Contact [16]) and HLLD (Harten-Lax-van Leer-Discontinuities [16]).

Here, we use HLLD solver. According to [16], this solver is more robust and efficient than the linearized Riemann solvers and with an equally good resolution. Besides, HLLD scheme is specially suitable in the treatment of problems which have contact discontinuities.

Figures 5 and 6 show, respectively, the form of the components v_x and v_y of the velocity considered in the simulation. The reader should note the initial configuration depicts a layer of fluid in the region $-0,5 < x < 0,5$ and which is moving along the positive direction of x-axis, while the outer layers are moving in the opposite direction. Besides, note that v_y plays the hole of the initial perturbations which will give rise to the instabilities.

We considered a Courant-Friedrichs-Levy number (CFL) like parameter as having the value 0.3. Such a parameter, which is related to the size of the time steps of the simulations in relation to the numerical domain partition [17], is a necessary condition to perform the numerical solutions of partial differential equations. In general form, $0.0 < CFL < 1.0$ for the advection equation and, the lower the number, the smaller the time steps considered by the code.

Figure 7 shows the time evolution of the density profiles and of the magnetic field vectors for the problems considered. In the left side we can observe the growing of the KH instabilities from the initial state for the case of the ideal MHD. From top to bottom, we plot the simulation at the instants 0.2, 0.4 and 0.6 s.

Note that the shape of the perturbations is similar to waves such as, for example, the sea surface

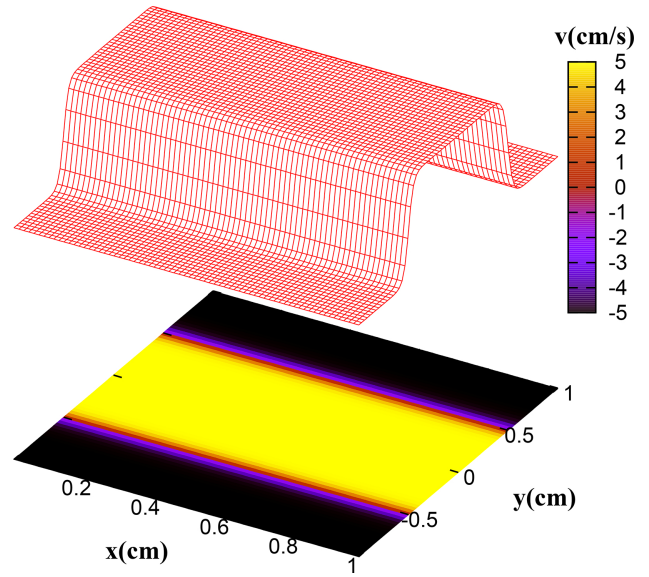


Figure 5: Component v_x of the velocity of the fluid.

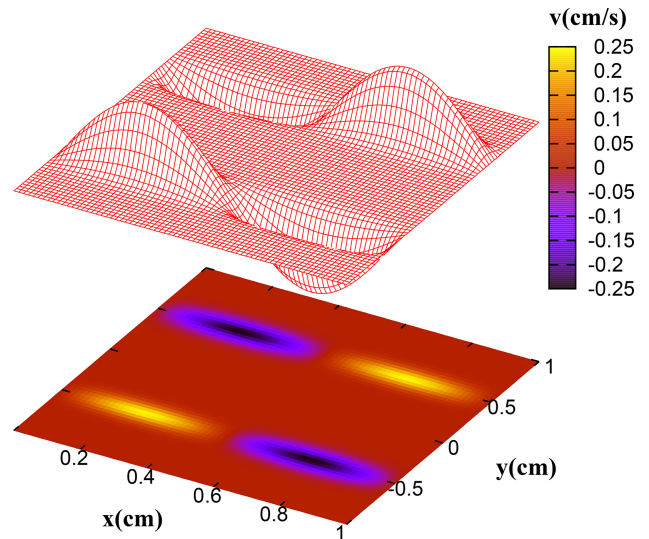


Figure 6: Same as in Fig. 5 for v_y .

waves discussed previously, although the present simulation depicts a more complex case. Such a fact indicate us how present that phenomenon is in the fluid mechanics.

Basically, if there are layers with different densities in tangential motion relative to each other, under certain circumstances the KH instabilities can arise along the interfaces between two of such layers. In this simulation, the given circumstance is a small perturbation acting as a “seed”.

The right side of Fig. 7 shows the simulation for the case of the resistive MHD, that is, where the resistivity of the system cannot be neglected.

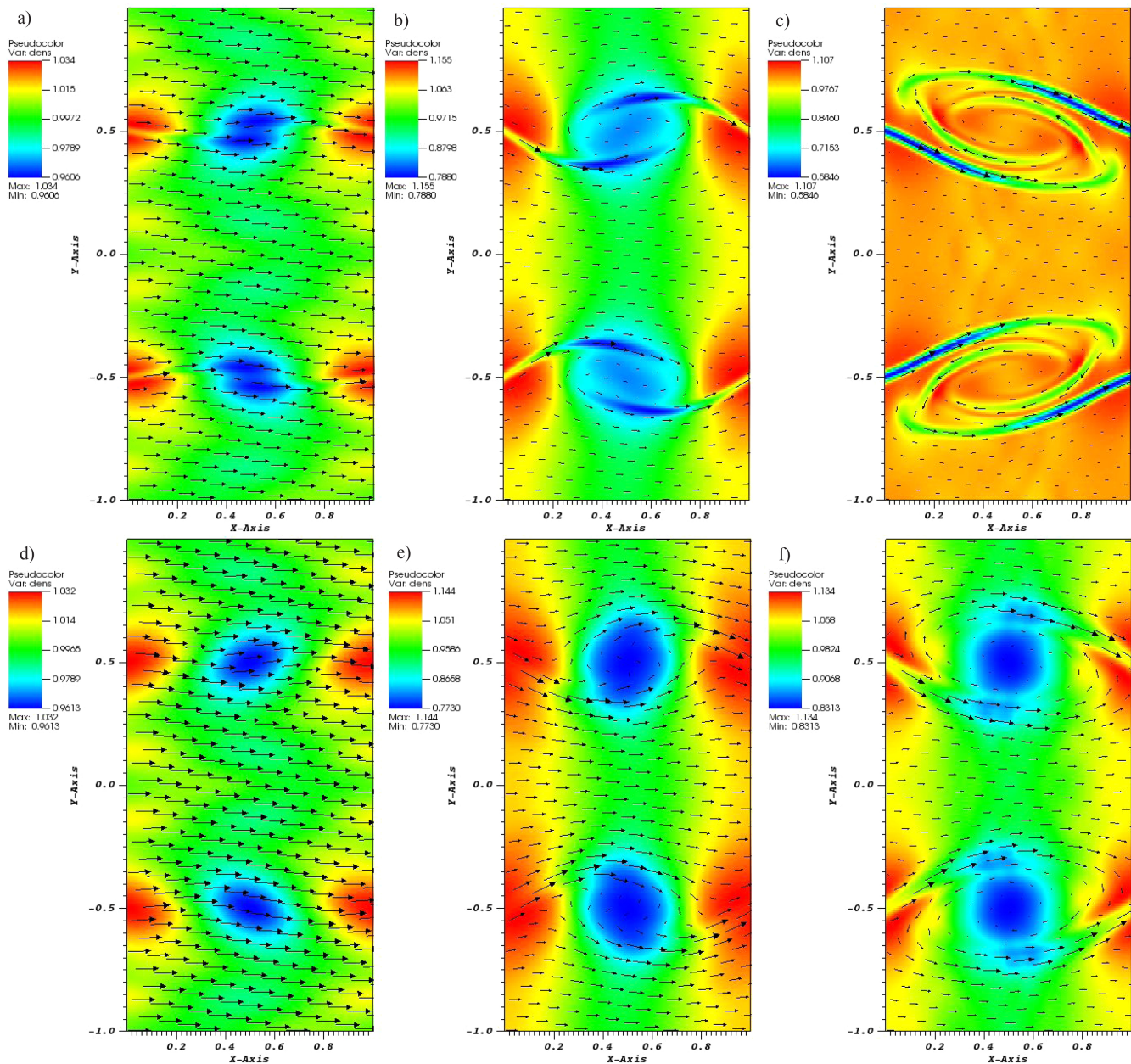


Figure 7: Simulations at 0.2, 0.4, 0.6 seconds (from left to right) showing the density profile for the case of ideal (a, b, c) and non-ideal (d, e, f) MHD, where we have a magnetic resistivity different from zero. Vectors represent the magnetic field.

Particularly, we gave the resistivity η the value¹ $\eta = 0.02$ s. Again, from top to bottom, we depict the evolution of the system at the instants 0.2, 0.4 and 0.6 s. Comparing this simulation to the one corresponding to the ideal MHD, we can note that the main effect of the finite resistivity is “slowing” the time evolution of the instabilities.

Further, it is worth pointing out the behavior of the magnetic field in both cases. Note that it tends

to remain “attached” to the flux. Such a behavior is typical of the MHD. Nevertheless, as it is mentioned in Section 2, in some cases that “attachment” can be broken in the reconnection processes.

5. Conclusions

In this paper we discussed some aspects of the MHD. Particularly, we shown the basic formalism of the ideal MHD, besides mentioning its non-ideal forms, such as the resistive MHD. Of particular importance in this issue are the instabilities which, as we can

¹It is an interesting fact that in CGS units the resistivity is given in seconds.

deduce from the discussions, surge in several forms and under many circumstances.

By means of three examples we shown that such instabilities are important in the study of several processes in space physics. More specifically, we discussed the existence of the KH and the MR instabilities in Crab nebula and in accretion disks, respectively. As the third example, we presented the phenomenon of magnetic substorms in Earth's magnetosphere, where the magnetic reconnection plays an important role.

From the basic equations of the hydrodynamics we deduced an analytic approach to the KH instabilities. We shown as such an instability arise at the interface between two layers of different densities and which have tangential motion relative to each other. Although the deductions are based only in the equations of the hydrodynamics, we observed that such a phenomenon is intrinsically related to the MHD.

As an example, we used FLASH code in order to create the simulation of a specific case of KH instability. Generally speaking, the code creates the simulations from the framework of the MHD and it consider some particular characteristics for each type of problem. However, we noted that, fundamentally, the phenomenon is the same that the simplified, analytic one deduced in Section 4. This fact pointed to the universality of the process. Further, in the simulations, we studied the difference in the results when using the ideal and the resistive MHD. We observed that the resistivity has the main effect of "slowing" the time evolution of the KH instabilities.

FLASH Code

FLASH code, developed by University of Chicago², is a very useful tool in the simulation of the MHD problems. What makes the FLASH specially suitable for handling the MHD problems is the fact of having schemes for solving the equations which are useful in the treatment of the magnetic reconnection problems found, for example, in solar physics, as well as problems involving fluxes undergoing magnetic perturbations. The latter are typical of astrophysical events such as accretion processes in neutron stars and black holes [18].

The latest version of the code, named FLASH4, has two different algorithms for solving the MHD

equations. Specifically, such algorithms solve the equations for the ideal and non-ideal cases in one, two and three dimensions.

The first algorithm is the eight-wave model [5]; the second one is the unsplit staggered mesh (USM) [19]. There are significant differences between the two methods, and one of them is the manner how each scheme deals with the zero-divergence condition of the magnetic field.

The eight-wave model uses the truncation-error method, which is efficient in removing the non-physical effects due to the magnetic monopoles in the cases where these are generated during the simulation. On the other hand, the USM uses the method called constrained transport [20], which manages to maintain the magnitude of $\nabla \cdot \mathbf{B}$ of order of 10^{-12} in the most of the simulations.

The second difference which is worth mentioning is the fact the USM uses the unsplit algorithm to evolve the system of equations, while the eight-wave uses the split method. The latter has the advantage of being robust and of a relatively simple implementation. However, the split algorithm introduces errors when handling some classes of problems, making the unsplit scheme an interesting choice in some cases.

Acknowledgements

E.F.D. Evangelista thankfully acknowledges financial support from Brazilian agency CNPq (grant 158967/2014-3); M.O. Domingues, O. Mendes and O.D. Miranda thankfully acknowledge Brazilian agencies CNPq, CAPES and FAPESP.

References

- [1] V.C.A. Ferraro and C. Plumpton, *An Introduction to Magneto-Fluid Mechanics* (Clarendon Press, Oxford, 1966).
- [2] C. Foullon, E. Verwichte, V.M. Nakariakov, K. Nykyri and C.J. Farrugia, *Astrophys. J. Lett.* **729**, L8 (2011).
- [3] D.H. Sharp, *Physica D* **12**, 3 (1984).
- [4] M.O. Domingues, A.K.F. Gomes, S.M. Gomes, O. Mendes, B. Di Pierro and K. Schneider, *ESAIM Proceed* **43**, 95 (2013).
- [5] K.G. Powell, P.L. Roe, T.J. Linde, T.I. Gombosi and D.L. De Zeeuw, *J. Comput. Phys.* **154**, 284 (1999).
- [6] W.K. Panofsky and M. Phillips, *Classical Electricity and Magnetism* (Addison-Wesley, Reading, 1962).

²<http://flash.uchicago.edu/site/flashcode>

- [7] J. Birn and E.R. Priest (eds), *Reconnection of Magnetic Fields* (Cambridge University Press, New York, 2007).
- [8] D. Biskamp, *Nonlinear Magnetohydrodynamics: Cambridge Monographs on Plasma Physics* (Cambridge University Press, Cambridge, 1993).
- [9] O. Porth, S.S. Komissarov and R. Keppens, *Mon. Not. R. Astron. Soc.* **443**, 547 (2014).
- [10] B.W. Carroll and D.A. Ostlie, *An Introduction to Modern Astrophysics* (Addison-Wesley, San Francisco, 2007), 2nd ed.
- [11] S.A. Balbus and J.F. Hawley, *Astrophys. J.* **376**, 214 (1991).
- [12] W.H. Campbell, *Introduction to Geomagnetic Fields* (Cambridge University Press, Cambridge, 2003), 2nd ed.
- [13] S. Chandrasekhar, *Hydrodynamic and Hydromagnetic Stability* (Oxford University Press, London, 1961).
- [14] A. Dedner et al., *J. Comput. Phys.* **175**, 645 (2002).
- [15] P.L. Roe, *J. Comp. Phys.* **43**, 357 (1981).
- [16] F. Miyoshi and K. Kusano, *J. Comp. Phys.* **208**, 315 (2005).
- [17] J. Vides, E. Audit, H. Guillard and B. Nkonga, *ESAIM Proceed.* **43**, 180 (2013).
- [18] A. Dubey, L.B. Reid and R. Fisher, *Phys. Scripta* **T132**, 014046 (2008).
- [19] D. Lee and A.E. Deane, *J. Comp. Phys.* **228**, 952 (2009).
- [20] C.R. Evans and J.F. Hawley, *Astrophys. J.* **332**, 659 (1988).